Supplement for "VOCs Emissions, Evolutions and Contributions to SOA Formation at a Receptor Site in Eastern China"

B. Yuan[1*], W.W. Hu[1**], M. Shao[1], M. Wang[1], W.T. Chen[1], S.H. Lu[1], L.M. Zeng[1], M. Hu[1]

1. *State Joint Key Laboratory of Environmental Simulation and Pollution Control, College of Environmental Sciences and Engineering, Peking University, Beijing, 100871, China.*

**now at: Earth System Research Laboratory, Chemical Sciences Division, NOAA, 325 Broadway, Boulder, Colorado 80305, USA*

***now at: Cooperative Institute for Research in Environmental Sciences, University of Colorado, Boulder, CO 80309, USA*

1. Correction of acetic acid measured by PTR-MS

Measurements of acetic acid by PTR-MS at m/z 61 have been investigated by many studies (Haase et al., 2012 and the references therein). No significant interference was observed in urban plumes (de Gouw et al., 2003), biomass burning plumes (Christian et al., 2004) and rural environments (Haase et al., 2012). However, PTR-MS measurements in Mexico City showed that ethyl acetate from industrial emissions can also fragment to m/z 61 channel (Fortner et al., 2009). Ethyl acetate can also produce m/z 89 and m/z 43 in PTR-MS (Fortner et al., 2009). Laboratories tests show that ethyl acetate fragment to m/z 61 at 65.7%, m/z 43 at 23.0% and most of the remaining signal is at m/z 89 (11.3%). Fragmentation of ethyl acetate in our PTR-MS is significantly higher than the PTR-MS used by *Fortner et al.* (2009) during the MILAGRO campaign, possibly due to the larger E/N (133 Td) of our PTR-MS than that of TA&MU PTR-MS (115 Td) (Fortner et al., 2009).

Acetic acid concentrations ($[AA]$) during the Changdao campaign are calculated as:

$$[AA]=\frac{I_{m61}-I_{m89}\times R}{S} \qquad \text{(Eq. S-1)}$$

Here, I_{m61} and I_{m89} are the normalized signals of m/z 61 and m/z 89, respectively. R is the ratio of m/z 61 versus m/z 89 from ethyl acetate (5.58). S is the sensitivity of acetic acid at m/z 61 and is determined from the calibration of acetic acid using permeation tube method. Fig. S1 show the scatterplots of acetic acid with m/z 61 concentrations. Acetic acid accounted for 67.1% of m/z 61 concentrations during the campaign. During the two biomass burning plumes, the contributions from acetic acid in m/z 61 were 74.2% and 85.8%, respectively. The large percentages of acetic acid in m/z 61 are consistent with high emissions of acetic acid from biomass burning (Akagi et al., 2011).

2. Time series of VOCs, CO and meteorological parameters

Fig. S3 shows time series of CO, VOCs species and meteorology parameters from April 2 to April 25, 2011. The Changdao campaign was conducted in the transit period between winter and spring. Temperature varied in the range of 0-20 °C and the average temperature was 9.9±3.8 °C. Temperature was strongly depended on the large-scale weather system. As the cold fronts invaded the northern China with strong winds from north direction, temperature dropped dramatically and the concentrations of various air pollutants decreased. When cold front was on the wane and the wind directions turned to south or southwest, air masses from Shandong Peninsula and Beijing-Tianjin regions brought higher VOCs and CO concentrations to Changdao site.

From April 2 to the noon on April 3, concentrations of pollutants were low in this period. Starting from the afternoon on April 3, the wind came from south and southwest and the pollutants increased dramatically. This pollution episode persisted to April 10 when the wind direction turned back to northeast and north. Two periods with high concentrations of pollutants were recorded: April 4 and April 7. A new pollution episode occurred from April 11. The concentrations of benzene and CO in this episode were significantly lower than those on April 4 and April 7, whereas the concentrations of some OVOCs species (e.g. acetone) reached the maximum in the campaign. From April 16 to April 20, the concentration of pollutants maintained at low levels though the wind directions changed several times. A new round of cold front swept north China starting from the noon of April 21 and temperature decreased by 8-10 °C. On April

22, northwestern wind arrived at Changdao site and the pollutants increased significantly. Another important feature during this period was the high relative humidity.

3. Calculation of NO_3 concentrations

The main source of NO_3 in the atmosphere is the reaction of NO_2 with ozone:

$$NO_2 + O_3 \rightarrow NO_3 + O_2 \cdot \qquad \text{(Eq. S-2)}$$

The rate coefficient of the above reaction ($k_{NO_2+O_3}$) is 3.2×10^{-17} cm^3 $molecule^{-1}$ s^{-1}. Thus, the formation rate of NO_3 (P_{NO_3}) could be expressed by:

$$P(NO_3) = k_{NO_2+O_3}[NO_2][O_3] \qquad \text{(Eq. S-3)}$$

NO_3 has a temperature-dependent equilibrium with N_2O_5 in the atmosphere.

$$NO_2 + NO_3 \Leftrightarrow N_2O_5 \qquad \text{(Eq. S-4)}$$

The loss pathways of NO_3 radical in the atmosphere include photolysis, reaction with NO, reactions with VOCs species and the indirect losses of N_2O_5, which reacts with H_2O and other components on the surface of ambient aerosol.

NO_3 is efficiently photolyzed in sunlight through the two different pathways:

$$NO_3 + h\nu \rightarrow NO_2 + O \ (90\%) \qquad \text{(Eq. S-5)}$$

$$NO_3 + h\nu \rightarrow NO + O_2 \ (10\%) \qquad \text{(Eq. S-6)}$$

The first pathway is more important. Photolysis frequency of NO_3 is expressed as J_{NO_3}.

The reaction of NO_3 and NO is:

$$NO_3 + NO \rightarrow NO_2 + NO_2 \qquad \text{(Eq. S-7)}$$

The rate constant of this reaction (k_{NO_3+NO}) is 2.7×10^{-11} cm^3 $molecule^{-1}$ s^{-1}。

NO_3 can also react with many VOCs species, including anthropogenic emitted ethene, propene and biogenic isoprene and monoterpenes. The rate constants of various VOCs species with NO3 are expressed as $k_{NO_3+VOC_i}$.

If the losses of NO_3 due to aerosol uptake and indirect losses of N_2O_5 are not considered, the loss rate of NO_3 could be shown as:

$$L_{NO_3} = (J_{NO_3} + k_{NO_3+NO}[NO] + \sum_i k_{NO_3+VOC_i}[VOC]_i) \quad \text{(Eq. S-8)}$$

Assuming the steady state of NO_3 concentration in the atmosphere, NO_3 concentrations could be expressed as:

$$[NO_3] = \frac{k_{NO_2+O_3}[NO_2][O_3]}{J_{NO_3} + k_{NO+NO_3}[NO] + \sum_i k_{NO_3+VOC_i}[VOC]_i} \quad \text{(Eq. S-9)}$$

Since L_{NO_3} is the lower limit of the total loss rates of NO_3, Eq. S-9 overestimates NO_3 concentrations in the atmosphere. The uncertainty of calculated NO_3 concentration come from measurement uncertainties of NO, NO_2, O_3, different VOCs species, NO_3 photolysis frequency and reaction rate coefficients used in Eq. S-9. Another important uncertainty source is the contribution of NO_3 and N_2O_5 heterogenic losses to NO_3 sink. The contributions vary significantly among different environments and different sites (25%-80% for polluted regions) (Brown et al., 2011). The calculation of NO_3 sinks from Eq. S-8 show that reaction with NO is the most important pathway for NO_3 losses, due to high NO concentrations (0.9±1.2 ppb) in this study. Thus, NO_3 and N_2O_5 heterogenic losses to aerosol should only be important when NO is low at night (J_{NO3} is also low). These calculated NO_3 data points may be overestimated by 33%-400% using the reported contributions of NO_3 and N_2O_5 heterogenic losses.

4. Calculation of OVOC photolysis frequencies

Besides the reactions with the three oxidants, OVOC species can also undergo photolysis in the atmosphere. The photolysis frequencies of OVOC species are scaled from the measured photolysis frequency of NO2 (J_{NO_2}) and calculated photolysis frequency of NO2 ($J_{NO_2,calculated}$) and OVOCs ($J_{OVOC,calculated}$) from parameterization equations using the solar zenith angle (SZA) as input information (Eq. 4) (Saunders et al., 2003). The determined formaldehyde photolysis frequencies show good agreements with measured values from the photometer, with a slope of 0.966 and a correlation coefficient (R) of 0.998.

$$J_{OVOC} = J_{NO_2} \times \frac{J_{NO_2,calculated}}{J_{OVOC,calculated}} \quad \text{(Eq. S-10)}$$

Tables

Table S1. Rate constants of VOCs species with OH radical, ozone and NO_3 radical used in this study.

Species	k_{OH}, $\times10^{-12}$ cm^3 molecule^{-1} s^{-1}	k_{O3}, $\times10^{-17}$ cm^3 molecule^{-1} s^{-1}	k_{NO3}, $\times10^{-14}$ cm^3 molecule^{-1} s^{-1}
Ethane	0.248	0	0.001
Ethene	8.52	0.159	0.0.05
Propane	1.09	0	0.007
Propene	26.3	1.01	0.945
i-Butane	2.12	0	0.0106
n-Butane	2.36	0	0.00459
Acetylene	0.85	0	0.0051
t-2-Butene	56.4	19	39
1-Butene	31.4	0.964	1.35
i-Butene	51.4	0.964	1.35
c-2-Butene	64.0	12.5	35.2
i-Pentane	3.60	0	0.0162
n-Pentane	3.80	0	0.0087
1,3-Butadiene	66.6	0.63	10
1-pentene	31.4	1.06	1.5
trans-2-pentene	67.0	16	37
isoprene	101	1.27	70
cis-2-pentene	65.0	13	37
2,2-dimethylbutane	2.23	0	0.044
2,3-dimethylbutane	5.78	0	0.044
2-methylpentane	5.40	0	0.018
cyclopentane	4.97	0	0.014
3-methylpentane	5.20	0	0.022
1-hexene	37.0	1.31	1.8
n-hexane	5.20	0	0.011
2,4-dimethylpentane	4.77	0	0.015
methylcyclopentane	5.20	0	0.014
2-methylhexane	5.65	0	0.015
Cyclohexane	6.97	0	0.014
2,3-dimethylpentane	1.50	0	0.015
3-methylhexane	5.60	0	0.015
Benzene	1.22	<0.001	0.003
2,2,4-trimethylpentane	3.34	0	0.009
n-heptane	6.76	0	0.015
Methylcyclohexane	4.97	0	0.014

Species	k_{OH}, $\times 10^{-12}$ cm^3 molecule^{-1} s^{-1}	k_{O3}, $\times 10^{-17}$ cm^3 molecule^{-1} s^{-1}	k_{NO3}, $\times 10^{-14}$ cm^3 molecule^{-1} s^{-1}
2,3,4-trimethylpentane	6.60	0	0.019
2-methylheptane	7.00	0	0.019
3-methylheptane	7.00	0	0.019
Toluene	5.63	<0.001	0.007
n-octane	8.11	0	0.019
Ethylbenzene	7.00	<0.001	0.06
m,p-xylene	18.9	<0.001	0.038
n-Nonane	9.70	0	0.023
o-xylene	13.6	<0.001	0.041
styrene	58.0	1.7	150
i-Propylbenzene	6.30	<0.001	0.06
n-Propylbenzene	5.80	<0.001	0.06
m-ethyltoluene	11.8	<0.001	0.086
p-ethyltoluene	18.6	<0.001	0.086
n-decane	11.0	0	0.028
1,3,5-trimethylbenzene	56.7	<0.001	0.088
o-ethyltoluene	11.9	<0.001	0.086
1,2,4-trimethylbenzene	32.5	<0.001	0.18
1,2,3-trimethylbenzene	32.7	<0.001	0.19
1,3-Diethylbenzene		<0.001	
1,4-Diethylbenzene		<0.001	
Naphthalene	24.4	<0.02	
α-pinene	52.3	8.4	616
β-pinene	74.3	1.5	251
Acetonitrile	0.02		
Acetaldehyde	15	<0.001	0.27
Propanal	20	<0.001	0.65
Butanal	24	<0.001	1.1
Pentanal	28	<0.001	1.5
Methanol	0.94	<0.001	0.013
Acetone	0.17	<0.001	<0.003
MEK	1.22	<0.001	
3-Pentanone	2	<0.001	
2-Pentanone	4.4	<0.001	
Formic Acid	0.4		
Acetic Acid	0.8		
Acrolein	18.3		0.33
MACR	29	0.12	0.34
MVK	20	0.52	<0.06

105 a. Data are from Atkinson and Arey (2003), Atkinson et al. (2006), Atkinson et al. (1983) and Salgado et
106 al. (2008).

107

Table S2. Mixing ratio of gases and meteorological parameters at Changdao

Parameters (ppb)	Unit	Average±Stdev
O3	ppb	43±15
NO	ppb	0.9±1.2
NO2	ppb	15.3±7.1
CO	ppb	563±428
Temperature	°C	9.9±3.8
RH	%	57.3±20.5
Pressure	kPa	101.2±0.6
Wind speed	m/s	4.6±2.2

Table S3. SOA yields of aromatics under different circumstances of high-NOx condition and the parameters for calculating SOA yields.

Species	α_1	C_1*, μg /m^3	α_2	C_2*, μg /m^3	SOA yield (OA, μg/m^3; T, K)			
					OA=15 T=273	OA=15 T=283	OA=50 T=273	OA=50 T=283
Benzene	0.072	0.30	0.888	111.1	0.355	0.264	0.613	0.498
Toluene	0.058	2.32	0.113	21.3	0.136	0.121	0.158	0.150
m-xylene	0.031	1.31	0.09	34.5	0.084	0.072	0.106	0.098
Naphthalene[a]	0.21	1.69	1.07	270.3	0.376	0.308	0.626	0.501

a:Values are from *Chan et al.* (2009) and values of other species are from *Ng et al.* (2007).

Table S4. Calculated SOA formation from PAHs basing on emission characteristics of coal burning reported in the literatures.

Type	NAP, mg/kg[a]	Other PAHs, mg/kg[a]	Other PAHs/NAP, g/g	SOA from other PAHs, $\mu g/m^3$ /ppm CO	
				Low-NOx	High-NOx
Beijing Honeycomb	1.6	2.94	1.84	1.220	0.652
Taiyuan Honey comb	5.8	7.25	1.25	0.829	0.443
Taiyuan Chunk	14	41.38	2.96	1.961	1.048
Yulin Chunk #1	13	112.39	8.65	5.738	3.066
Yulin Chunk #2	11	60.78	5.52	3.667	1.959

a: Data is from *Shen et al.* (2010). Units are the PAHs emissions mass from burning of 1 kg coal.

Table S5. Calculated SOA from PAHs basing on emission characteristics of biomass burning reported in the literatures.

Type	Fuel	NAP, mg/kg	Other PAHs, mg/kg	Other PAHs/NAP, g/g	SOA from other PAHs, μg/m^3 /ppm CO	
					Low-NOx	High-NOx
Flamming	Wheat[a]	108.8	89.6	0.820	0.547	0.292
	Horsebean	51.9	2.8	0.053	0.035	0.018
	Horsebean	16.9	5.7	0.337	0.223	0.119
	Peanut	22.3	5.4	0.240	0.159	0.085
	Soybean	12.6	5.0	0.400	0.265	0.141
	Soybean	16.2	6.7	0.416	0.276	0.147
	Cotton	19.3	6.8	0.354	0.234	0.125
	Cotton	32.6	8.9	0.272	0.18	0.096
	Rice	53.5	11.9	0.223	0.148	0.079
	Rice	41.2	10.7	0.259	0.171	0.091
	Wheat	62.7	13.4	0.214	0.141	0.075
	Wheat	34.2	7.3	0.215	0.142	0.076
	Rape	64.5	15.7	0.244	0.161	0.086
	Rape	49.5	15.5	0.313	0.207	0.11
	Sesame	12.4	4.9	0.399	0.265	0.141
	Sesame	11.3	2.8	0.248	0.164	0.088
	Corn	25.8	8.9	0.346	0.229	0.122
	Corn	40.0	10.3	0.258	0.17	0.091
Smoldering	Horsebean	6.4	2.0	0.318	0.211	0.112
	Horsebean	12.1	4.1	0.338	0.224	0.119
	Peanut	22.7	7.5	0.329	0.218	0.116
	Soybean	28.2	7.8	0.275	0.182	0.097
	Soybean	20.8	6.2	0.296	0.196	0.105
	Cotton	17.4	5.5	0.316	0.209	0.112
	Cotton	3.8	0.9	0.231	0.153	0.081
	Rice	23.3	4.2	0.181	0.119	0.064
	Rice	48.6	8.4	0.173	0.114	0.061
	Wheat	21.0	12.5	0.597	0.396	0.211
	Wheat	41.3	8.3	0.202	0.134	0.071
	Rape	11.1	2.0	0.178	0.118	0.063
	Rape	28.4	8.5	0.298	0.198	0.105
	Sesame	6.3	2.9	0.462	0.306	0.163
	Sesame	4.5	1.5	0.332	0.22	0.117
	Corn	7.1	1.7	0.238	0.158	0.084
	Corn	12.3	3.3	0.264	0.175	0.093

a: Data is from *Zhang et al.* (2008) for biomass burning, and other values are from *Shen et al.* (2011). Units are the PAHs emissions mass from burning of 1 kg crop straw.

Table S6. Emission ratios of aromatics to CO at two sites (Guangzhou and Panyu) in PRD

Species	Guangzhou, ppb/ppm[a]	Panyu, ppb/ppm[a]
Benzene	1.73	2.04
Toluene	5.37	6.32
Ethylbenzene	1.29	1.52
m+p-xylene	1.92	2.38
o-xylene	0.94	1.16
1,2,4-TMB	0.69	0.629

a: values are calculated from emission ratios of aromatics to acetylene (Tang et al., 2007) and emission ratio of acetylene to CO (4.9 ppb/ppm) (Barletta et al., 2008).

Figures

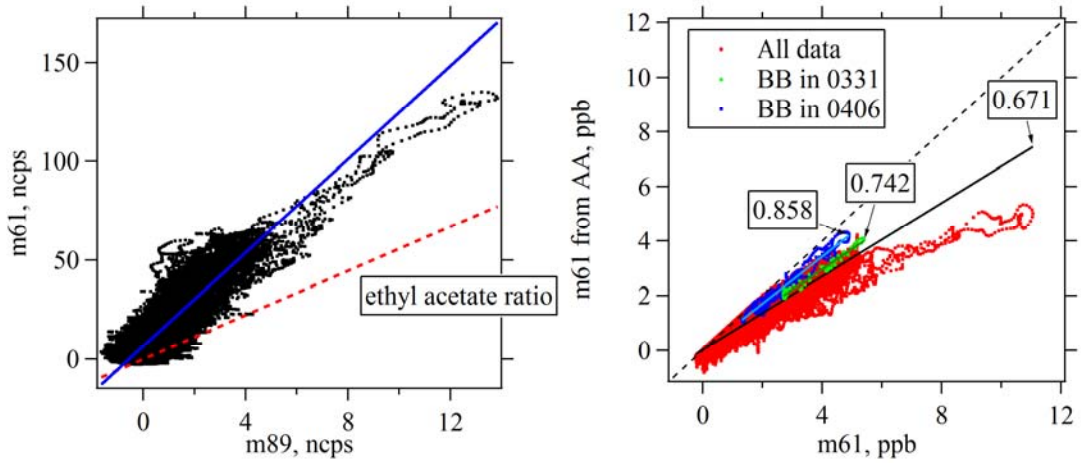

Fig. S1. Correction of acetic acid measurements using signal of m/z 89. (Left) Scatterplots of the normalized signal of m/z 61 with m/z 89. The dashed red line is the ratio of m/z 61 and m/z 89 in the spectrum of ethyl acetate in PTR-MS. The blue line is the linear fit of the data points during the whole Changdao campaign. (Right) Scatterplots of m/z 61 concentrations from acetic acid with m/z 61 concentrations (red dots). The black line is the linear fit of data points during the whole campaign. The dashed black line indicates 1:1 relationship. The green and blue dots and lines are the two biomass burning plumes on 31 March and 6 April, respectively. The numbers in the two boxes are calculated slopes of the lines.

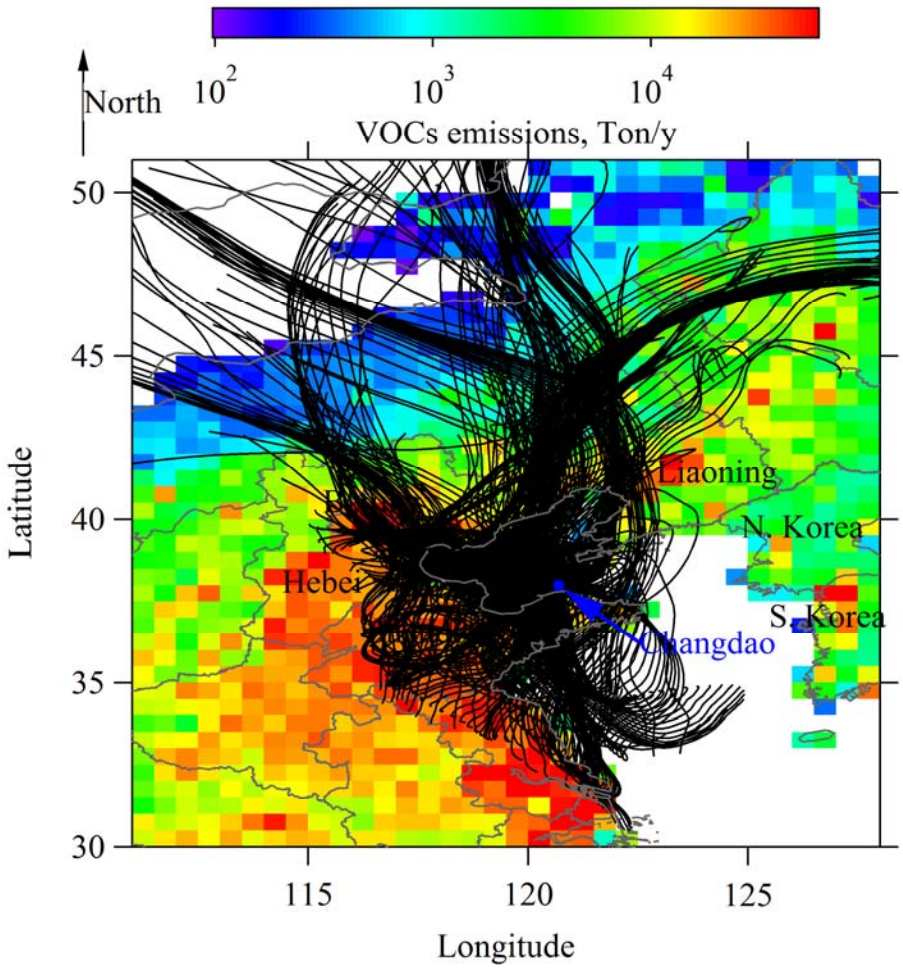

Fig. S2. Hourly back trajectories of Changdao site during the campaign. The areas are color-coded using VOCs emissions strength (Zhang et al., 2009).

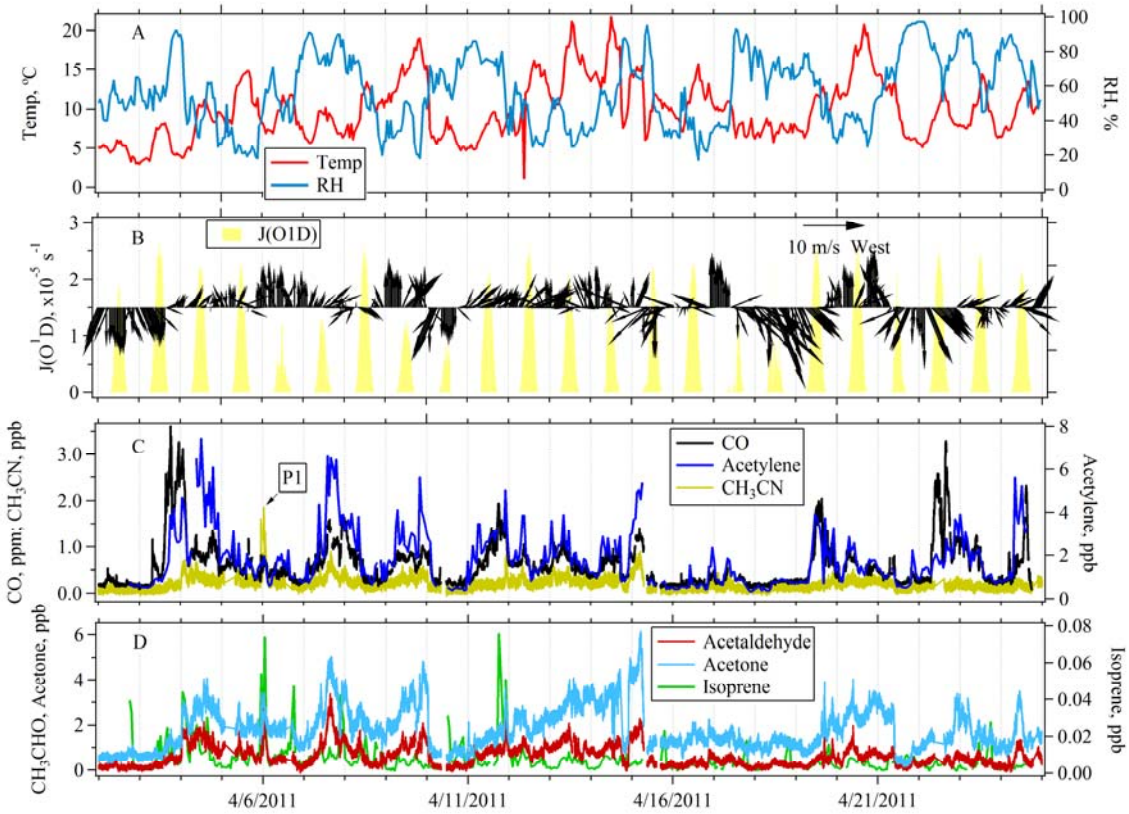

Fig. S3. Time series of several VOCs species and other meteorological parameters. A: temperature (red), relative humidity (dark blue); B: $J(O^1D)$ (light yellow), wind speed and direction (black); C: CO (black), acetylene (blue), acetonitrile (dark yellow); D: acetaldehyde (dark red), acetone (light blue), isoprene (green).

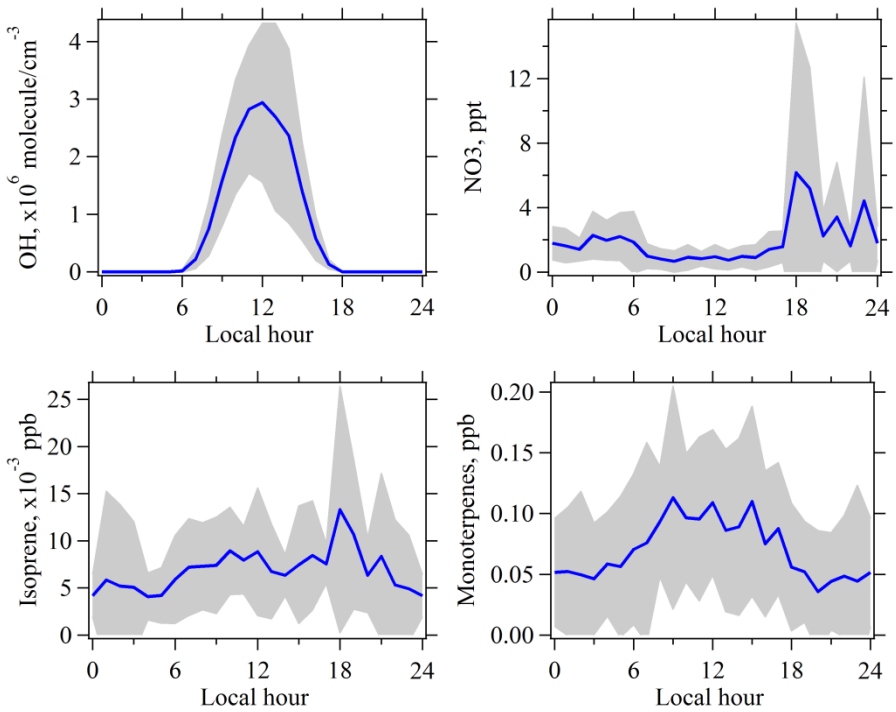

Fig. S4. Diurnal profile of calculated OH and NO3 concentration and measured isoprene and monoterpene concentrations. The shaded area show the standard deviations.

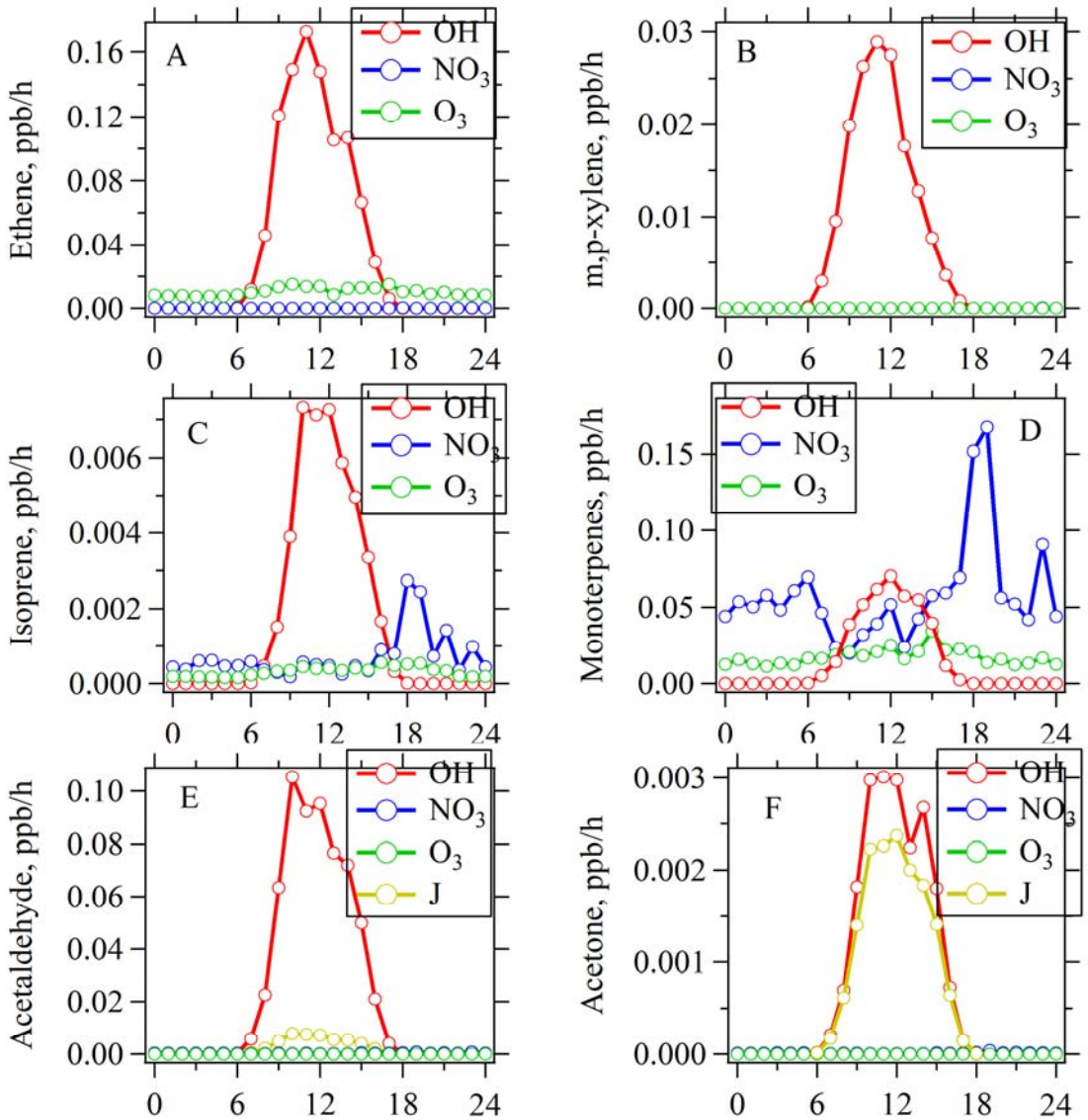

Fig. S5. Diurnal variations of VOCs loss rates due to the reactions with OH radical (red lines), NO_3 radical (blue lines) and ozone (green lines). The losses due to photolysis (brown lines) for OVOCs species (acetaldehyde and acetone) are also included in the graphs.

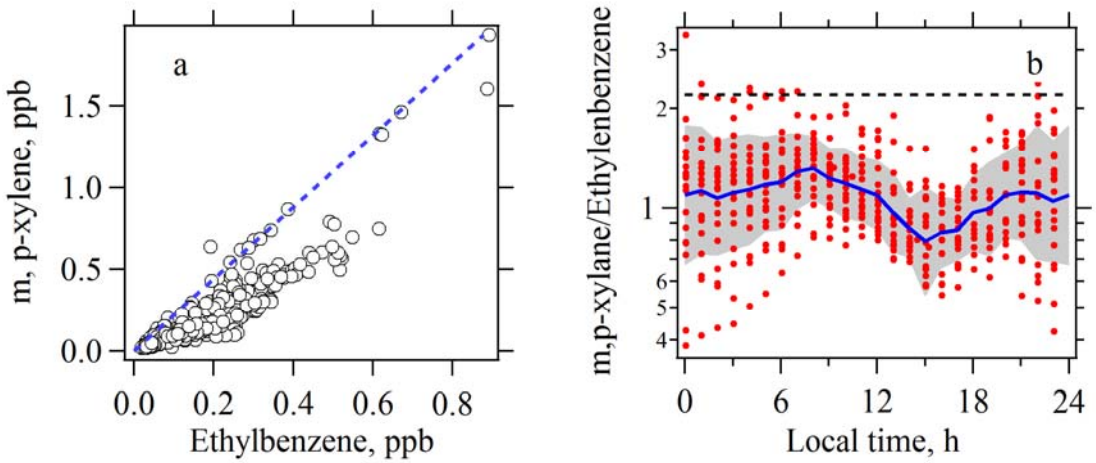

Fig. S6. Scatterplots of m+p-xylene with ethylbenzene (a) and diurnal variations of m+p-xylene/ethylbenzene ratio (b) during the Changdao Campaign. The blue line and grey areas in (b) are geometric averages and standard deviations, respectively. Red dots are the measured concentration ratios. The blue dashed line in (a) and black dashed line in (b) indicate the selected the initial emission ratio of m+p-xylene to ethylbenzene.

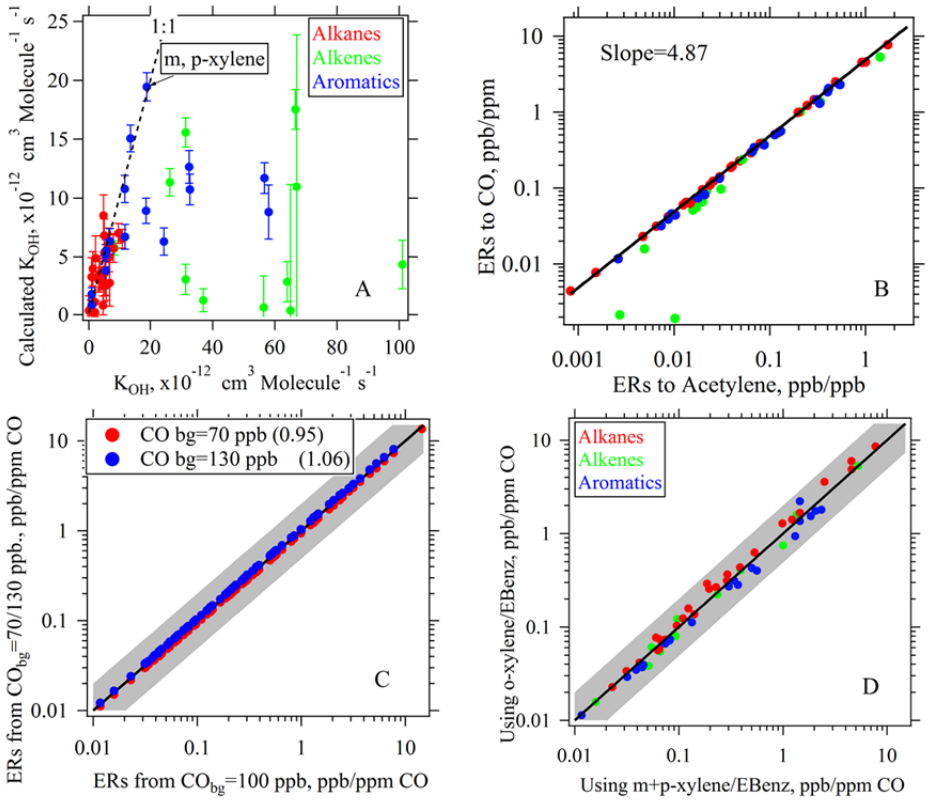

Fig. S7. (A) Comparison of the calculated k_{OH} from Eq. 5 with the values in the literature. The dashed line shows the 1:1 relationship. (B) Scatterplots of the calculated VOCs emission ratios calculated using CO as urban tracer with those calculated using acetylene as urban tracer. The black line is the linear fit to the data points. The slope (4.87) is close to the regression line from the scatterplot of acetylene with CO (4.30). (C) Comparison of calculated emission ratios of NMHCs to CO using CO background concentrations of 100 ppb, 70 ppb and 130 ppb. (D) Comparison of emission ratios of NMHCs to CO using m+p-xyelne/ethylbenzene ratio and o-xylene /ethylbenzene ratio to calculate photochemical age. The black lines (in C and D) indicate the 1:1 relationship, and the gray areas (in C and D) show agreements within a factor of two.

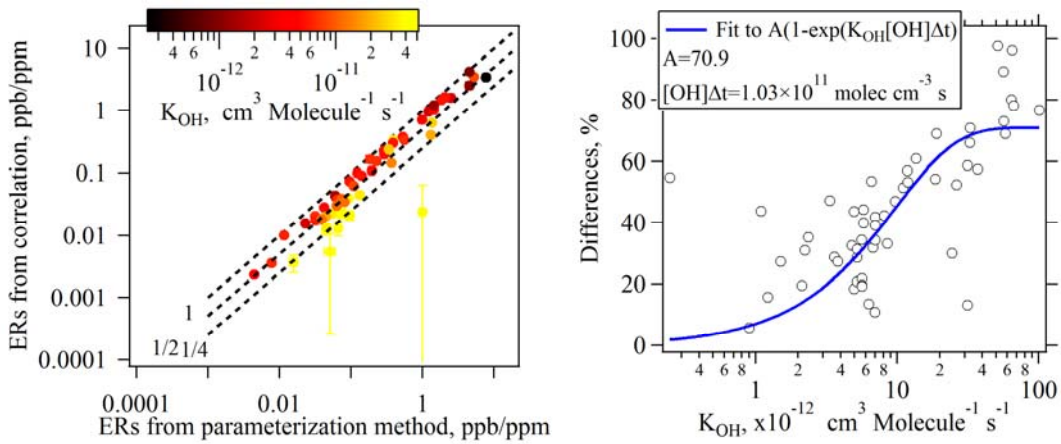

Fig. S8. (left) Comparison the emission ratios determined from photochemical age based parameterization method with those from linear regressions. The dots are color-coded according to k_{OH} values of hydrocarbons. (right) Scatterplot of the difference of emission ratios between the two methods ($1-\frac{ER_{\text{linear regresssion}}}{ER_{\text{parameterization}}}$) with k_{OH} values of hydrocarbons. The blue line is the fit result from the data points using this equation: Difference=A×(1-exp(k_{OH}[OH]Δt) (de Gouw et al., 2009).

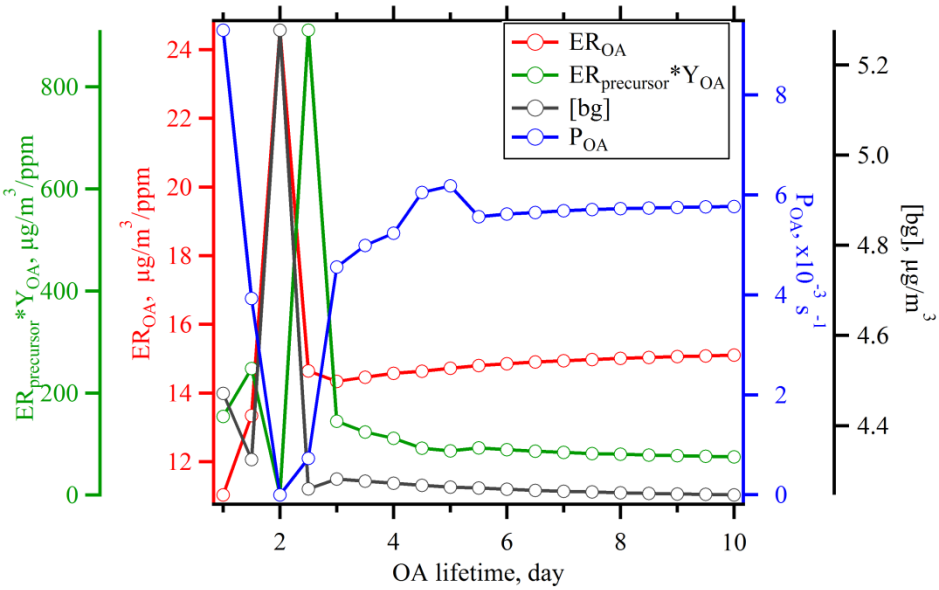

Fig. S9. Variations of the parameters from the fitting of OA concentrations, as varying the assumed OA lifetime.

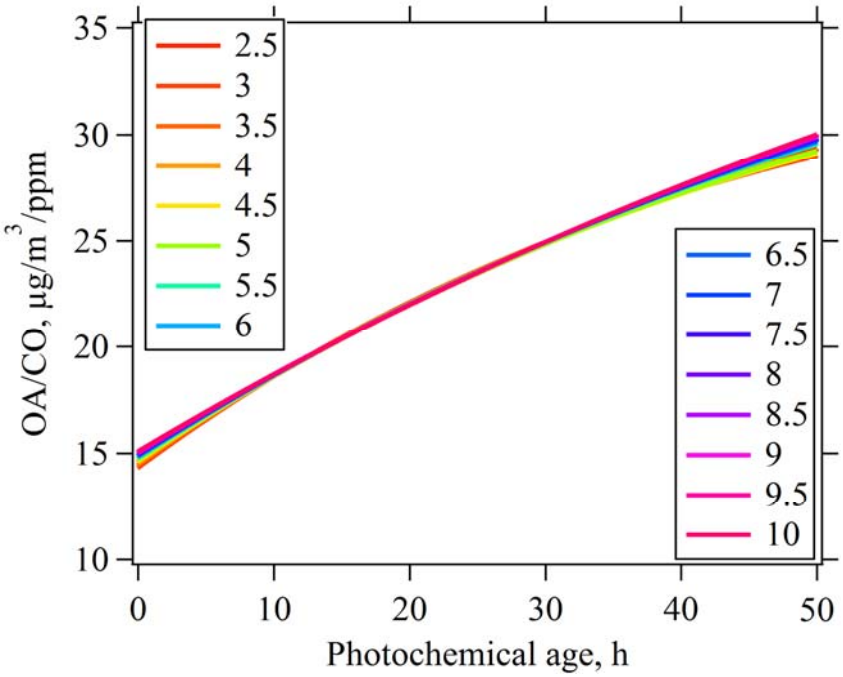

Fig. S10. The dependence of OA/CO ratio with photochemical age, as varying the assumed OA lifetimes. The numbers in the legend are the OA lifetime in days for each curve.

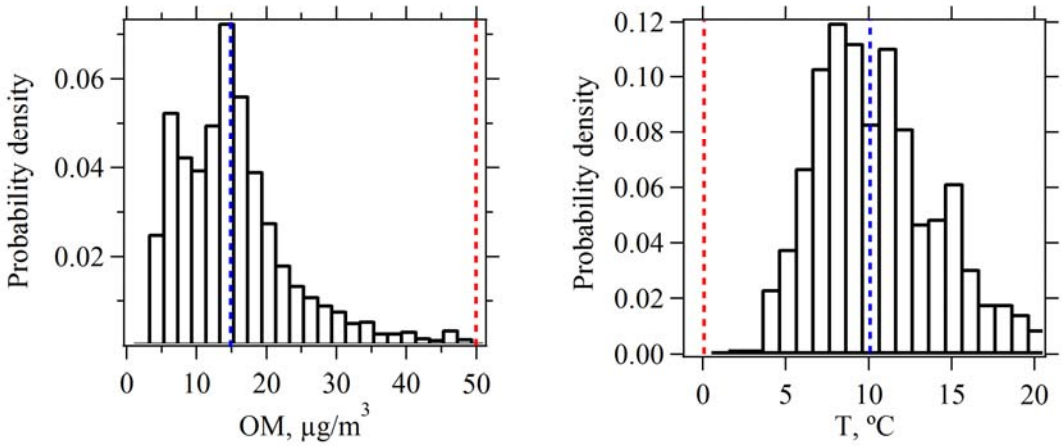

Fig. S11. Histograms of the concentrations of organic aerosol (left) and temperature (right). The blue lines in the two graphs indicate an OM concentration of 15 μg/m^3 and a temperature of 10 °C, whereas red lines indicate an OM concentration of 50 μg/m^3 and a temperature of 0 °C.

Reference:

Akagi, S. K., Yokelson, R. J., Wiedinmyer, C., Alvarado, M. J., Reid, J. S., Karl, T., Crounse, J. D., and Wennberg, P. O.: Emission factors for open and domestic biomass burning for use in atmospheric models, Atmos. Chem. Phys., 11, 4039-4072, 10.5194/acp-11-4039-2011, 2011.

Atkinson, R., and Arey, J.: Atmospheric degradation of volatile organic compounds, Chemical Reviews, 103, 4605-4638, Doi 10.1021/Cr0206420, 2003.

Atkinson, R., Baulch, D. L., Cox, R. A., Crowley, J. N., Hampson, R. F., Hynes, R. G., Jenkin, M. E., Rossi, M. J., and Troe, J.: Evaluated kinetic and photochemical data for atmospheric chemistry: Volume II - gas phase reactions of organic species, Atmospheric Chemistry and Physics, 6, 3625-4055, 2006.

Atkinson, R., Aschmann, S. M., and Pitts, J. N.: Kinetics of the gas-phase reactions of OH radicals with a series of α,β-unsaturated carbonyls at 299 ± 2 K, International Journal of Chemical Kinetics, 15, 75-81, 10.1002/kin.550150108, 1983.

Barletta, B., Meinardi, S., Simpson, I. J., Zou, S. C., Rowland, F. S., and Blake, D. R.: Ambient mixing ratios of nonmethane hydrocarbons (NMHCs) in two major urban centers of the Pearl River Delta (PRD) region: Guangzhou and Dongguan, Atmospheric Environment, 42, 4393-4408, DOI 10.1016/j.atmosenv.2008.01.028, 2008.

Brown, S. S., Dubé, W. P., Peischl, J., Ryerson, T. B., Atlas, E., Warneke, C., de Gouw, J. A., te Lintel Hekkert, S., Brock, C. A., Flocke, F., Trainer, M., Parrish, D. D., Feshenfeld, F. C., and Ravishankara, A. R.: Budgets for nocturnal VOC oxidation by nitrate radicals aloft during the 2006 Texas Air Quality Study, J. Geophys. Res., 116, doi:10.1029/2011JD016544, 10.1029/2011jd016544, 2011.

Christian, T. J., Kleiss, B., Yokelson, R. J., Holzinger, R., Crutzen, P. J., Hao, W. M., Shirai, T., and Blake, D. R.: Comprehensive laboratory measurements of biomass-burning emissions: 2. First intercomparison of open-path FTIR, PTR-MS, and GC- MS/FID/ECD, Journal of Geophysical Research-Atmospheres, 109, D02311, doi:02310.01029/02003JD003874, 10.1029/2003jd003874, 2004.

de Gouw, J. A., Goldan, P. D., Warneke, C., Kuster, W. C., Roberts, J. M., Marchewka, M., Bertman, S. B., Pszenny, A. A. P., and Keene, W. C.: Validation of proton transfer reaction-mass spectrometry (PTR-MS) measurements of gas-phase organic compounds in the atmosphere during the New England Air Quality Study (NEAQS) in 2002, Journal of Geophysical Research-Atmospheres, 108, doi:10.1029/2003JD003863, 10.1029/2003jd003863, 2003.

de Gouw, J. A., Welsh-Bon, D., Warneke, C., Kuster, W. C., Alexander, L., Baker, A. K., Beyersdorf, A. J., Blake, D. R., Canagaratna, M., Celada, A. T., Huey, L. G., Junkermann, W., Onasch, T. B., Salcido, A., Sjostedt, S. J., Sullivan, A. P., Tanner, D. J., Vargas, O., Weber, R. J., Worsnop, D. R., Yu, X. Y., and Zaveri, R.: Emission and chemistry of organic carbon in the gas and aerosol phase at a sub-urban site near Mexico City in March 2006 during the MILAGRO study, Atmospheric Chemistry and Physics, 9, 3425-3442, 2009.

Fortner, E. C., Zheng, J., Zhang, R., Knighton, W. B., Volkamer, R. M., Sheehy, P., Molina, L., and Andre, M.: Measurements of Volatile Organic Compounds Using Proton Transfer Reaction - Mass Spectrometry during the MILAGRO 2006 Campaign, Atmospheric Chemistry and Physics, 9, 467-481, 2009.

Haase, K. B., Keene, W. C., Pszenny, A. A. P., Mayne, H. R., Talbot, R. W., and Sive, B. C.: Calibration and intercomparison of acetic acid measurements using proton transfer reaction mass

spectrometry (PTR-MS), Atmos. Meas. Tech. Discuss., 5, 4635-4665, 10.5194/amtd-5-4635-2012, 2012.

Salgado, M. S., Monedero, E., Villanueva, F., Martín, P., Tapia, A., and Cabañas, B.: Night-Time Atmospheric Fate of Acrolein and Crotonaldehyde, Environmental Science & Technology, 42, 2394-2400, 10.1021/es702533u, 2008.

Saunders, S. M., Jenkin, M. E., Derwent, R. G., and Pilling, M. J.: Protocol for the development of the Master Chemical Mechanism, MCM v3 (Part A): tropospheric degradation of non-aromatic volatile organic compounds, Atmos. Chem. Phys., 3, 161-180, 10.5194/acp-3-161-2003, 2003.

Schauer, J. J., Kleeman, M. J., Cass, G. R., and Simoneit, B. R. T.: Measurement of Emissions from Air Pollution Sources. 2. C1 through C30 Organic Compounds from Medium Duty Diesel Trucks, Environmental Science & Technology, 33, 1578-1587, 10.1021/es980081n, 1999.

Shen, G., Wang, W., Yang, Y., Zhu, C., Min, Y., Xue, M., Ding, J., Li, W., Wang, B., Shen, H., Wang, R., Wang, X., and Tao, S.: Emission factors and particulate matter size distribution of polycyclic aromatic hydrocarbons from residential coal combustions in rural Northern China, Atmospheric Environment, 44, 5237-5243, 10.1016/j.atmosenv.2010.08.042, 2010.

Shen, G., Wang, W., Yang, Y., Ding, J., Xue, M., Min, Y., Zhu, C., Shen, H., Li, W., Wang, B., Wang, R., Wang, X., Tao, S., and Russell, A. G.: Emissions of PAHs from Indoor Crop Residue Burning in a Typical Rural Stove: Emission Factors, Size Distributions, and Gas−Particle Partitioning, Environmental Science & Technology, 45, 1206-1212, 10.1021/es102151w, 2011.

Tang, J. H., Chan, L. Y., Chan, C. Y., Li, Y. S., Chang, C. C., Liu, S. C., Wu, D., and Li, Y. D.: Characteristics and diurnal variations of NMHCs at urban, suburban, and rural sites in the Pearl River Delta and a remote site in South China, Atmospheric Environment, 41, 8620-8632, DOI 10.1016/j.atmosenv.2007.07.029, 2007.

Zhang, Y., Dou, H., Chang, B., Wei, Z., Qiu, W., Liu, S., Liu, W., and Tao, S.: Emission of Polycyclic Aromatic Hydrocarbons from Indoor Straw Burning and Emission Inventory Updating in China, Annals of the New York Academy of Sciences, 1140, 218-227, 10.1196/annals.1454.006, 2008.